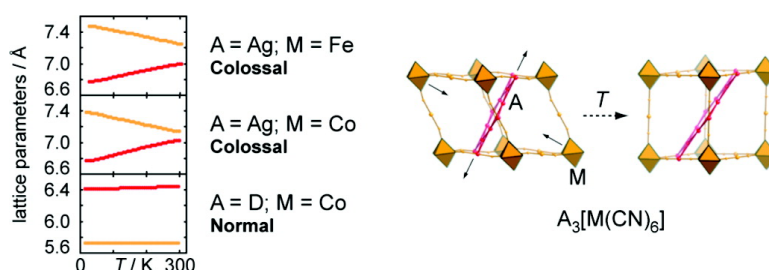


## Argentophilicity-Dependent Colossal Thermal Expansion in Extended Prussian Blue Analogues

Andrew L. Goodwin, David A. Keen, Matthew G. Tucker,  
 Martin T. Dove, Lars Peters, and John S. O. Evans

*J. Am. Chem. Soc.*, **2008**, 130 (30), 9660-9661 • DOI: 10.1021/ja803623u • Publication Date (Web): 03 July 2008

Downloaded from <http://pubs.acs.org> on February 8, 2009



### More About This Article

Additional resources and features associated with this article are available within the HTML version:

- Supporting Information
- Links to the 1 articles that cite this article, as of the time of this article download
- Access to high resolution figures
- Links to articles and content related to this article
- Copyright permission to reproduce figures and/or text from this article

[View the Full Text HTML](#)

## Argentophilicity-Dependent Colossal Thermal Expansion in Extended Prussian Blue Analogues

Andrew L. Goodwin,<sup>\*,†</sup> David A. Keen,<sup>‡,§</sup> Matthew G. Tucker,<sup>‡</sup> Martin T. Dove,<sup>†</sup> Lars Peters,<sup>⊥</sup> and John S. O. Evans<sup>⊥</sup>

Department of Earth Sciences, University of Cambridge, Downing Street, Cambridge CB2 3EQ, U.K., ISIS Facility, Rutherford Appleton Laboratory, Harwell Science and Innovation Campus, Didcot, Oxfordshire OX11 0QX, U.K., Department of Physics, University of Oxford, Clarendon Laboratory, Parks Road, Oxford OX1 3PU, U.K., and Department of Chemistry, University Science Laboratories, University of Durham, South Road, Durham DH1 3LE, U.K.

Received May 15, 2008; E-mail: alg44@cam.ac.uk

Metallophilic interactions are recognized as one of the most important supramolecular bonding motifs, capable of producing a range of fascinating physical, structural, and chemical effects.<sup>1</sup> As a means of directing molecular and framework topologies, recent applications include the syntheses of metallomacrocylic Möbius strips and interwoven Borromean sheets, metallophilicity-driven guest inclusion in metallocryptands, and even the spontaneous resolution of homochiral coordination polymers.<sup>2</sup> The design of reversible RGB-color switches has exploited their tunable phosphorescence,<sup>3</sup> just as their electronic sensitivity to chemical environment and temperature has led to the development of vapochromic, spin-crossover, photoreactive, and rotator phases.<sup>4</sup>

We have recently reported “colossal” thermal expansion in  $\text{Ag}_3[\text{Co}(\text{CN})_6]$  [**1**],<sup>5</sup> a flexible framework material that contains layers of Ag atoms connected via argentophilic interactions. The material is remarkable because, when heated, its structure expands and contracts (in different directions) at rates more than ten times greater than the usual positive thermal expansion of “normal” materials. What is not yet clear is whether this highly unusual behavior can be attributed to extreme geometric flexibility of its covalent lattice or whether metallophilic interactions also play a key role. Resolving this issue is of fundamental importance because it may help understand a wealth of unusual temperature-dependent effects in other systems containing these interactions.

Here we show that argentophilicity is required for colossal thermal expansion in **1**. Our approach is to study compositional variants with the same structure type, and hence with similar geometric flexibility, but with  $\text{Ag}\cdots\text{Ag}$  interactions sometimes retained and sometimes absent. Comparison of the thermal expansion behavior of these materials then provides a method of assessing the roles of flexibility, argentophilicity, and chemical composition in the “colossal” behavior of **1**. We use X-ray and neutron powder diffraction experiments to measure thermal expansion in two key  $\text{A}_3[\text{M}(\text{CN})_6]$  variants:  $\text{Ag}_3[\text{Fe}(\text{CN})_6]$  [**2**] and  $\text{D}_3[\text{Co}(\text{CN})_6]$  [**3**]. Previous reports of the structure of **3** at 293 and 77 K led us to anticipate that it would not show colossal expansion;<sup>6</sup> however, the absence of expansivity data for Ag-containing analogues such as **2**, or indeed any extensive data for **3** precluded any conclusion as to the role of  $\text{Ag}\cdots\text{Ag}$  interactions.

Compounds **1–3** crystallize with a trigonal structure in which octahedrally coordinated  $\text{M}^{\text{III}}$  ions are connected in a linear fashion by pentanuclear  $\text{CN}-\text{A}^1-\text{NC}$  bridges.<sup>7–9</sup> The framework structure formed is topologically equivalent to the cubic  $\alpha$ -Po network of

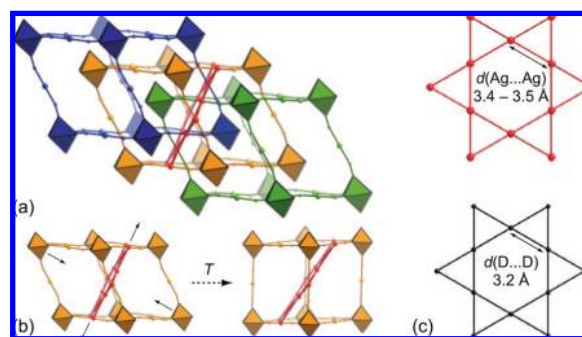


**Figure 1.** Representations of the crystal structure of the  $\text{A}_3[\text{M}(\text{CN})_6]$  extended Prussian blue framework (a) and the contraction along the trigonal axis toward the ideal cubic framework (b) effected by expansion of the Kagome Ag/D lattices (c).  $[\text{MC}_6]$  polyhedra are given as filled octahedra and  $-\text{N}-\text{Ag}/\text{D}-\text{N}-$  linkages in ball and stick representation.

the Prussian blues, but in this case the network is sufficiently open to allow 3-fold interpenetration (Figure 1a) along a unique body diagonal of the Prussian-blue-like “cages”. The structures of all three compounds are extended along this axis, such that the  $\text{Ag}^+$  or  $\text{D}^+$  cations in perpendicular planes are brought together to form Kagome nets with relatively short  $\text{Ag}\cdots\text{Ag}$  or  $\text{D}\cdots\text{D}$  distances (Figure 1c). Expansion within these planes makes the Prussian blue cages more upright if the covalent  $\text{M}-\text{CN}-\text{A}-\text{NC}-\text{M}$  bond lengths are preserved (Figure 1b).

The thermal expansion behavior of each phase was measured using X-ray and neutron powder diffraction to monitor the lattice parameters as a function of temperature (Figure 2). In all cases, the  $a$  lattice parameter is exactly twice the separation between neighboring atoms in the Kagome sheets, while the  $c$  parameter is directly proportional to the elongated cube diagonal. The “ideal” cube geometry occurs for  $c = a\sqrt{2}$ . Data were collected on cooling from room temperature to  $\sim 10$  K; no phase transitions were observed (including magnetic transitions in the case of **2**). Coefficients of thermal expansion are shown in the bottom panels of Figure 2, and mean values obtained via linear fits to the lattice parameter data are listed in Table 1. What is immediately evident is that **2** exhibits colossal thermal expansion behavior similar to **1** (i.e.,  $|\alpha| \geq 100 \text{ MK}^{-1}$ ), while the thermal expansion effects in **3** are an order of magnitude less extreme and hence not atypical for a framework material. Consequently, chemical variation at the octahedral transition metal site does not have any qualitative bearing on the thermal expansion behavior, while substitution at the Ag site has a profound effect.

There is a remarkable similarity in the  $a$  unit cell parameters of compounds **1** and **2** at corresponding temperature points. This is

<sup>†</sup> University of Cambridge.  
<sup>‡</sup> Rutherford Appleton Laboratory.  
<sup>§</sup> University of Oxford.  
<sup>⊥</sup> University of Durham.

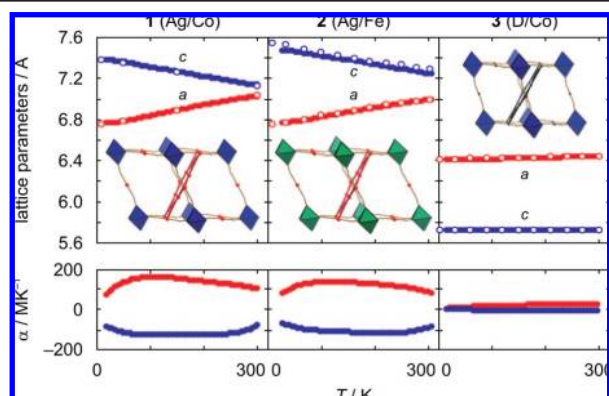


**Figure 2.** Temperature-dependent cell parameters (top) and thermal expansion coefficients (bottom) of the  $A_3[M(CN)_6]$  family from neutron (open circles) and X-ray (filled circles) powder diffraction data.

**Table 1.** Mean  $A_3[M(CN)_6]$  Coefficients of Thermal Expansion ( $\alpha_a = \partial \ln(a)/\partial T$ ;  $\alpha_c = \partial \ln(c)/\partial T$ ) from Neutron and X-ray Powder Diffraction

compound	$\alpha_a^a$ (MK <sup>-1</sup> )	$\alpha_c^a$ (MK <sup>-1</sup> )	T (K)
1	+144(9)	-126(4)	10 → 300
2	+124.0(10)	-113(3)	8 → 310
3	+17.4(6)	-5.04(24)	8 → 304

<sup>a</sup> The errors in the values of  $\alpha$  given are from the least-squares linear fits to the data over the specified temperature range; these errors neglect any systematic experimental effects and subtle non-linearities of behavior.

in contrast to the  $c$  parameter values, which, despite varying with temperature in a similar way for both compounds, differ by 0.11 Å. This suggests that the  $a$  lattice parameter is determined by the ideal  $Ag \cdots Ag$  separation at each temperature, a value which might be expected to remain unchanged with variation at the octahedral transition metal site. The increased size of the  $Fe^{3+}$  cation ( $d_{Fe^{III}-C} = 1.92$  Å;  $d_{Co^{III}-C} = 1.86$  Å) is then accommodated via distortion along the cube diagonal; i.e., increasing  $c$ . As in many hexacyanoferrate(III) salts<sup>10</sup> we found some evidence for a slow autoreduction process in **2** whereby  $Fe^{3+}$  is reduced by cyanide to  $Fe^{2+}$ . Aged samples showed a decrease in the value of  $c$  (note that one expects<sup>10</sup>  $d_{Fe^{II}-CN} < d_{Fe^{III}-CN}$ ), and a slightly more moderate thermal expansion behavior as network connectivity is progressively reduced with time (data not shown).

The framework structure of **3** is closer to the ideal cube geometry than that of either **1** or **2**. This need not affect the flexibility of the framework, since variation in the cube angle can still occur.<sup>11</sup> Instead the geometries reflect a considerable difference in N–D and N–Ag bond lengths.<sup>12</sup> The contrasting behavior of **3** relative to that of Ag-containing analogues **1** and **2** is a strong indication that some property of the Ag atoms is responsible for the colossal thermal expansion effects.<sup>13</sup> One might reasonably expect that the vast difference between Ag and D atomic masses would only reduce thermal motion in **1** and **2** relative to **3**; moreover, density functional theory calculations show that the degree of covalency in Ag–N and D–N bonds is similar in these materials.<sup>14</sup> Consequently the evidence strongly suggests that  $Ag \cdots Ag$  interactions are responsible for the unusual behavior observed.

Finally, we note that marked temperature-dependent shifts in fluorescence energies have been observed in large families of other flexible framework materials containing  $Ag \cdots Ag$  or  $Au \cdots Au$  interactions.<sup>15</sup> Our work suggests that these spectroscopic observations might be understood in the context of very large thermal expansion effects; indeed, the two effects appear to be strongly coupled in  $K_2Na[Ag(CN)_2]_3$ .<sup>16</sup> On the basis of the apparent

generality of this unusual behavior, we anticipate that extreme thermal expansion may be a widespread property of flexible framework materials containing metallophilic interactions.

**Acknowledgment.** The authors thank H. Lewtas (Oxford University) for SQUID magnetometer measurements, Trinity College, Cambridge, for financial support to A.L.G. and EPSRC (U.K.) for financial support to J.S.O.E. and L.P. under ep/c538927/1.

**Supporting Information Available:** Details of neutron powder diffraction refinements and neutron and X-ray structural parameters. This material is available free of charge via the Internet at <http://pubs.acs.org>.

## References

- (1) (a) Schmidbaur, H. *Chem. Soc. Rev.* **1995**, 391–400. (b) Pyykkö, P. *Angew. Chem., Int. Ed.* **2004**, *43*, 4412–4456.
- (2) (a) Hui, S. C. F.; Huang, J.-S.; Sun, R. W.-Y.; Zhu, N.; Che, C.-M. *Angew. Chem., Int. Ed.* **2006**, *45*, 4663–4666. (b) Dobrzanska, L.; Raubenheimer, H. G.; Barbour, L. J. *Chem. Commun.* **2005**, 4970–4972. (c) Catalano, V. J.; Bennett, B. L.; Noll, B. C. *Chem. Commun.* **2000**, 1413–1414. (d) Chen, X. D.; Du, M.; Mak, T. C. W. *Chem. Commun.* **2005**, 4417–4419.
- (3) Kishimura, A.; Yamashita, T.; Aida, T. *J. Am. Chem. Soc.* **2005**, *127*, 179–185.
- (4) (a) Lefebvre, J.; Batchelor, R. J.; Leznoff, D. B. *J. Am. Chem. Soc.* **2004**, *126*, 16117–16125. (b) Galet, A.; Niel, V.; Muñoz, M. C.; Real, J. A. *J. Am. Chem. Soc.* **2003**, *125*, 14224–14225. (c) Elbjerrami, O.; Omary, M. A. *J. Am. Chem. Soc.* **2007**, *129*, 11384–11393. (d) Bachman, R. E.; Fioritto, M. S.; Fetcs, S. K.; Cocker, T. M. *J. Am. Chem. Soc.* **2001**, *123*, 5376–5377.
- (5) Goodwin, A. L.; Calleja, M.; Conterio, M. J.; Dove, M. T.; Evans, J. S. O.; Keen, D. A.; Peters, L.; Tucker, M. G. *Science* **2008**, *319*, 794–797.
- (6) (a) Güdel, H. U.; Ludi, A.; Fischer, P. *J. Chem. Phys.* **1972**, *56*, 674–675. (b) Haser, R.; de Broin, C. E.; Pierron, M. *Acta Crystallogr.* **1972**, *B28*, 2530–2537.
- (7) (a) Pauling, L.; Pauling, P. *Proc. Natl. Acad. Sci. U.S.A.* **1968**, *60*, 362–367. (b) Schröder, U.; Scholz, F. *Inorg. Chem.* **2000**, *39*, 10006–10016.
- (8)  $Ag_3[Co(CN)_6]$  and  $Ag_3[Fe(CN)_6]$  were prepared by reaction of aqueous solutions of  $AgNO_3$  (0.3 M, Aldrich) and either  $K_3[Co(CN)_6]$  or  $K_3[Fe(CN)_6]$  (0.1 M). The precipitates obtained were filtered, washed ( $H_2O$ ), and dried (50 °C, 24 h) to afford **1** and **2** as colourless and brick-red polycrystalline powders, respectively.  $D_3[Co(CN)_6]$  was obtained via repeated dissolution of  $H_3[Co(CN)_6]$  in  $D_2O$  (Aldrich) followed by solvent evaporation; the hydrogenous acid itself was isolated from  $K_3[Co(CN)_6]$  (Aldrich) via aqueous-phase ion exchange (Dowex 50W) and subsequent evaporation of solvent at 50 °C.
- (9) Neutron powder diffraction data were collected on the GEM instrument at ISIS: Hannon, A. C. *Nucl. Instrum. Methods Phys. Res. A* **2005**, *551*, 88–107. Approximately 3 g of each sample was placed within a cylindrical thin-walled V can (8 mm diameter, 5.8 cm height), mounted within a top-loading CCR. Data were corrected using standard methods (Dove, M. T.; Tucker, M. G.; Keen, D. A. *Eur. J. Mineral.* **2002**, *14*, 331–348). X-ray powder diffraction data were collected on a Bruker-AXS D8 diffractometer equipped with a Cu tube and Ni-filter. The diffractometer was operated in Bragg–Brentano geometry with the data collected using a LynxEye semiconductor strip detector. An Oxford Cryosystems phenix cryostat was used to control sample temperature, monitored using internal Al or Si standards. Each sample was dispersed as a finely ground powder onto a zero-background silicon wafer. Data collections were performed over the range  $10 \leq 2\theta \leq 75^\circ$  using a step size of  $\Delta 2\theta = 0.01^\circ$  and a counting time of 0.27 s/step. Structural refinements were carried out using the TOPAS package: Coelho, A. *TOPAS, General profile and structure analysis software for powder diffraction data*, version 2.0; Bruker AXS: Karlsruhe, Germany, 2000.
- (10) Sharpe, A. G. *The Chemistry of Cyano Complexes of the Transition Metals*; Academic: London, 1976.
- (11) The  $ac$  ratio in **1** at 500 K ( $a/c = 1.04$ , ref 5) is similar to that in **3** ( $a/c = 1.12$ ); hence, the geometry of **3** could allow “colossal” behaviour.
- (12) We explored the possibility, raised in previous studies, that the correct D atom site might be located away from the centre of the  $N \cdots N$  vector.<sup>6</sup> While our neutron Bragg diffraction data showed evidence for transverse vibrational motion (as might be anticipated) the best refinements placed the D atoms on the  $3g$  site ( $1/2, 0, 1/2$ ).
- (13) While thermal expansion behaviour scales with cell volume in, e.g., the  $A_2M_3O_{12}$  family (Evans, J. S. O.; Mary, T. A.; Sleight, A. W. *J. Solid State Chem.* **1997**, *133*, 580–583), a similar relationship here would give more extreme behaviour in **2** than **1**, which is not observed.
- (14) Calleja, M.; Goodwin, A. L.; Dove, M. T. *J. Phys.: Condens. Matter.* **2008**, *20*, 255226.
- (15) See, for example: Colis, J. C. F.; Laroche, C.; Staples, R.; Herbst-Irmer, R.; Patterson, H. H. *Dalton Trans.* **2005**, 1–5.
- (16) Laroche, C. L.; Omary, M. A.; Patterson, H. H.; Fischer, P.; Fauth, F.; Allenspach, P.; Lucas, B.; Pattison, P. *Solid State Commun.* **2000**, *114*, 155–160.

JA803623U